



Experimental study of sector and linear array ultrasound accuracy and the influence of navigated 3D-reconstruction as compared to MRI in a brain tumor model

Max Siekmann¹ · Thomas Lothes² · Ralph König³ · Christian Rainer Wirtz³ · Jan Coburger³

Received: 17 September 2017 / Accepted: 13 January 2018 / Published online: 24 January 2018
© CARS 2018

Abstract

Purpose Currently, intraoperative ultrasound in brain tumor surgery is a rapidly propagating option in imaging technology. We examined the accuracy and resolution limits of different ultrasound probes and the influence of 3D-reconstruction in a phantom and compared these results to MRI in an intraoperative setting (iMRI).

Methods An agarose gel phantom with predefined gel targets was examined with iMRI, a sector (SUS) and a linear (LUS) array probe with two-dimensional images. Additionally, 3D-reconstructed sweeps in perpendicular directions were made of every target with both probes, resulting in 392 measurements. Statistical calculations were performed, and comparative boxplots were generated.

Results Every measurement of iMRI and LUS was more precise than SUS, while there was no apparent difference in height of iMRI and 3D-reconstructed LUS. Measurements with 3D-reconstructed LUS were always more accurate than in 2D-LUS, while 3D-reconstruction of SUS showed nearly no differences to 2D-SUS in some measurements. We found correlations of 3D-reconstructed SUS and LUS length and width measurements with 2D results in the same image orientation.

Conclusions LUS provides an accuracy and resolution comparable to iMRI, while SUS is less exact than LUS and iMRI. 3D-reconstruction showed the potential to distinctly improve accuracy and resolution of ultrasound images, although there is a strong correlation with the sweep direction during data acquisition.

Keywords Neurosurgery · Ultrasound · Navigation · 3D-reconstruction · Phantom · Glioma

Introduction

The first line of treatment for gliomas is a neurosurgical operation. Multiple studies stress the importance of the extent of resection (EoR) on the survival for low-grade gliomas (LGG) and high-grade gliomas (HGG) [1–3]. To achieve this objective, a proper visualization and differentiation of tumor tissue and normal brain tissue is essential. In diffuse infiltrative gliomas, this can be especially challenging. Presently, there are several different imaging methods that can be used to visualize gliomas.

High-field intraoperative MRI with a field strength of 1.5T or 3T serves as the gold standard for intraoperative imaging as it shows comparable imaging results to pre- and postoperative MRI [4]. However, intraoperative MRI requires special regulations and standards for operation rooms which in turn create higher costs as well as increased time commitments for staff.

Intraoperative ultrasound (iUS) in contrast is inexpensive, allows fast image acquisition and is available in most

✉ Max Siekmann
max.siekmann@klinikum-nuernberg.de

Thomas Lothes
thomas.lothes@klinikum-kempton.de

Ralph König
ralph.koenig@uni-ulm.de

Christian Rainer Wirtz
Rainer.Wirtz@bkh-guenzburg.de

Jan Coburger
jan.coburger@uni-ulm.de

¹ Department of Traumatology and orthopedic surgery, Klinikum Nürnberg, Breslauer Straße 201, 90471 Nuremberg, Germany

² Department of Pediatrics, Klinikum Kempten, Robert-Weixler-Straße 50, 88439 Kempten, Germany

³ Department of Neurosurgery, University of Ulm, Campus Günzburg, Ludwig-Heilmeyer-Straße 2, 89312 Günzburg, Germany

neurosurgical centers [5]. For glioma surgery, it is a well-established and highly satisfying technique used in most centers performing glioma surgery [6]. In meta-analyses of studies using iUS for glioma resection, iUS was found to be of value for intraoperative resection guidance and can improve the extent of resection [7,8]. However, it has the disadvantages of providing only two-dimensional data and its subjective image interpretation leads to an abnormally high dependence on the expertise of the examiner [9,10].

New advances in ultrasound technology have been made and implemented into neurosurgical operation rooms. More than two-thirds of surgeons using iUS use some of these modern features [6]. Some clinical studies indicate a better orientation in the operation situs with navigated ultrasound probes [11]. Others demonstrate a better brain shift control with intraoperative data updates in modern navigated ultrasound [12–15]. In addition, first clinical studies using navigated ultrasound for resection control show divergent results, especially if they compare ultrasound to intraoperative MRI findings [9,16,17].

Apart from initial experience with the intraoperative navigated ultrasound and first clinical studies, to our knowledge there is no publicly available data investigating the technical possibilities of linear array ultrasound and its 3D-reconstruction compared with conventional sector array ultrasound and MRI with a special focus on accuracy and resolution limits. Both of these are crucial variables for brain tumor resection and resection control. Such data can only be provided by experimental trials.

We aim to evaluate the technical possibilities of modern linear array ultrasound (LUS) with and without 3D-reconstruction in an experimental study using phantoms. The results were compared to the current gold-standard MRI. On account of initial, promising clinical studies at our center [16, 17], we affirm that linear array transducers provide an accuracy and resolution comparable to that of intraoperative MRI.

Additionally, we investigated two-dimensional sector array ultrasound commonly used in brain surgery and the impact of 3D-reconstruction on the accuracy and resolution of this probe and compared the results to the findings of MRI.

As a third question, we compared the results of linear and sector array ultrasound (SUS). Taking into account the above-mentioned studies at our center [16,17], we expected the SUS results to be less exact than those of LUS and MRI.

Material and methods

Phantom

For this study, an agarose gel phantom was developed. The gel was cast in a defined cuboid acrylic glass mold with internal dimensions of 17.2 × 17 × 19 cm (height × width × length).

This mold functioned as an evaporation barrier and provided stability for the gel. To allow for optimal fusion and registration of any imaging method, donut markers and drill holes were placed on the exterior. The lower part of the mold was filled with an agarose and water mixture thus ultrasound reflections from the bottom of the mold could be avoided. In the upper 5.2 cm of the mold in every gel layer of 7.5 mm, bodies with defined dimensions (13 × 13 × 30 mm) were placed in defined angles to each other. Those bodies contained fine mica powder for contrasting them in MRI and ultrasound images and a higher concentration (3%) of agarose. The bodies were placed in pairs on the already congealed lower layer in angles of 1.91° and 5.73°. The angles are generated from a distance of one and three millimeters between the two bodies at one end of the fissure. The rectangular shape of the bodies was chosen to provide a straight fissure for easy and exact resolution measurements. These targets were then fixed with fine needles and cast into the next gel layer. Every layer contained four bodies and overlapped with the upper and lower layer. After seven of these layers, the top of the phantom was sealed with a thin foil without air pockets to prevent volume changes to the gel through evaporation. Two equal phantoms with 28 bodies each, forming 14 fissures for resolution measurements, were produced (Fig. 1).

Software and hardware

Except for the CT (*Philips® Brilliance 40 CT, Philips, Amsterdam, The Netherlands*), all devices were used in a *Brainsuite (Brainlab, Munich, Germany)* environment. This special operation room contained an optical ceiling-mounted navigation system (*VectorVision sky, Brainlab, Munich, Germany*), a 1.5 tesla MRI (*Espreo Magnetom, Siemens, Erlangen, Germany*) and a mobile ultrasound unit (*iU22, Philips*)

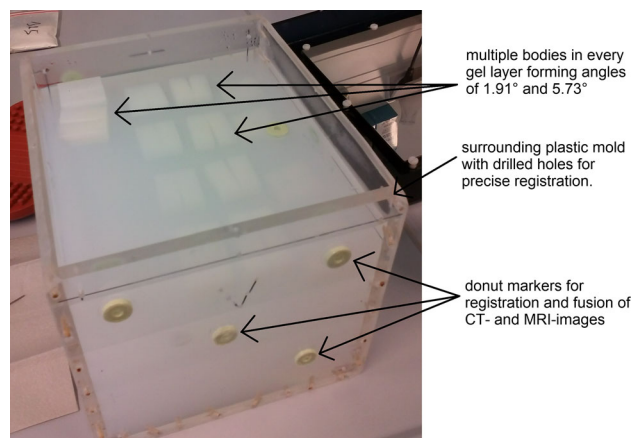


Fig. 1 View of the phantom during construction with attached donut markers and targets not yet fully embedded in agarose gel

in the same room. It was used with a *X7-2 xMATRIX* array transducer with a sector array image (SUS) and a *L15-7io* linear array transducer (LUS). The LUS was used with a *wideview* setting. It opened the field of view at the sides of the image by eight degrees, allowed the visualization of the upper five registration wires embedded in the registration phantom as required for an exact automated registration. Also, the full length of the bodies in the image plane could only be depicted with this setting enabled. Both probes used *XRES* (Philips) adaptive imaging processing. Penetration depth of LUS was set to 5 cm respectively 7 cm for the lowest target layer. SUS was set to 8.1 cm penetration depth. For navigation and registration *iPlan3.0* (Brainlab) was used.

Measurements

The phantom was first measured with CT (Philips® *Brilliance 40 CT*, Philips) set to the lowest possible slice thickness (0.488 mm) to get a highly accurate data set for navigation. This was necessary since the plastic mold with the drilled “anatomic landmarks” was not depicted in MRI images. Thereafter, it was placed into the 1.5 tesla *Siemens Espree Magnetom* (Siemens, Erlangen, Germany). The MRI scan was performed in a setting equal to an intraoperative MRI (iMRI). For the scan, a specialized head coil (Noras, H ochheim, Germany) was used. This head coil is typically used for intraoperative MRI. Hereafter, the phantom was referenced in the navigation system. Finally, the ultrasound probes were registered as described by Coburger et al. [18]. The above-described setup mimics the clinical situation of a cranial tumor surgery. Every target was measured with conventional two-dimensionally and three-dimensionally reconstructed ultrasound with the linear and sector ultrasound probe. The three-dimensional measures were taken twice: once with the image orientation parallel to the fissure between the bodies and once perpendicular to the fissure to determine whether any correlations of 3D-results and image acquisition direction exist or not (Fig. 2). For the reconstructed volumes, the software registered 30–50 ultrasound images with corresponding navigation data and calculated a 3D-volume. For measuring the smallest possible resolution with conventional ultrasound, trajectories were placed at the last point where the fissure was definable.

Statistics

Both distance and volumetric measurements of iMRI and the 3D-reconstructed ultrasound were taken with the *iPlan3.0* software. We took 2D measurements with LUS and SUS using the ultrasound device. Statistical calculations were performed with *SPSS 24* (Lead Technologies, INC, Charlotte, USA). Data were visualized using boxplots and tables. Cross-

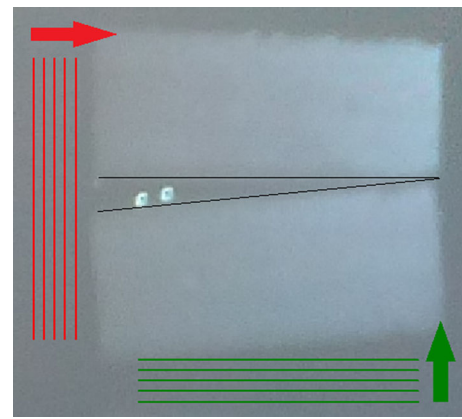


Fig. 2 Illustration of image orientation and sweep direction for 3D-data acquisition. Image of a target consisting of two bodies with the fissure (black) in between. Arrows mark the sweep direction, and the lines of the same color illustrate the image orientation. Red = image orientation perpendicular to the fissure (3D+ (+ representing the fissure and the image orientation with two perpendicular lines)), green = image orientation parallel to the fissure (3D= (= representing the fissure and the image orientation with two parallel lines)). The two white spots inside the fissure are light reflexes caused by the camera

correlating tables comparing the measurements against each other are provided in the supplements.

Results

Every target was measured once with each method. A total of 392 data sets were acquired: 56 data sets by iMRI, 56 two-dimensional data sets with each US-probe and 112 3D data sets for each US-probe. Half of these sets were made with an image plane parallel (3D=) and the other half with the image plane perpendicular (3D+) to the fissure formed by the angle between two bodies. Not all measurements were evaluable due to different issues described below. Table 1 shows the quantity of evaluable measurements for each body dimension as well as for resolution measurements.

iMRI magnetic resonance imaging in a setting equal to intraoperative MRI; *3D = LUS* 3-dimensional reconstructed linear array ultrasound with image plane parallel to the fissure; *3D+LUS* 3-dimensional reconstructed linear array ultrasound with image plane perpendicular to the fissure; *2DLUS* 2-dimensional linear array ultrasound; *3D = SUS* 3-dimensional reconstructed sector array ultrasound with image plane parallel to the fissure; *3D+SUS* 3-dimensional reconstructed sector array ultrasound with image plane perpendicular to the fissure; and *2DSUS* 2-dimensional sector array ultrasound.

Regarding the quantity of evaluable measurements, Table 1 reveals that sector ultrasound could never measure all targets for three reasons. Firstly, the image of the sector ultrasound probe with its pointed shape impeded a full acquisition of

Table 1 Results and quantity of evaluable measurements of all measurement methods

		iMRI	3D = LUS	3D+LUS	2DLUS	3D = SUS	3D+SUS	2DSUS
Length (real body dimension: 30 mm)	Evaluable measurements	56	40	56	48	24	48	32
	Mean value (in mm)	30.05	31.20	29.94	31.75	34.17	31.56	34.18
	Standard deviation (in mm)	0.20	0.50	0.33	0.33	0.63	1.05	0.54
	Mean relative difference to real body dimension (in %)	-0.2	-4.0	0.2	-5.9	-13.9	-5.2	-13.9
Height (real body dimension: 13 mm)	Evaluable measurements	56	56	56	56	48	48	48
	Mean value (in mm)	13.06	13.10	13.09	13.23	13.50	13.48	13.69
	Standard deviation (in mm)	0.21	0.15	0.14	0.18	0.30	0.31	0.27
	Mean relative difference to real body dimension (in %)	-0.5	-0.8	-0.7	-1.7	-3.9	-3.7	-5.3
Width (real body dimension: 13 mm)	Evaluable measurements	56	56	56	56	48	39	48
	Mean value (in mm)	12.91	12.76	13.05	13.25	13.78	14.65	14.59
	Standard deviation (in mm)	0.25	0.28	0.19	0.19	0.71	0.72	0.43
	Mean relative difference to real body dimension (in %)	0.7	1.8	-0.4	-2.0	-6.0	-12.7	-12.3
Resolution	Evaluable measurements	28	28	28	28	13	24	24
	Mean value (in mm)	0.28	0.33	0.15	0.57	1.26	0.66	1.07
	Standard deviation (in mm)	0.10	0.15	0.09	0.18	0.20	0.21	0.29

iMRI magnetic resonance imaging in a setting equal to intraoperative MRI; *3D = LUS* 3-dimensional reconstructed linear array ultrasound with image plane parallel to the fissure; *3D+LUS* 3-dimensional reconstructed linear array ultrasound with image plane perpendicular to the fissure; *2DLUS* 2-dimensional linear array ultrasound; *3D = SUS* 3-dimensional reconstructed sector array ultrasound with image plane parallel to the fissure; *3D+SUS* 3-dimensional reconstructed sector array ultrasound with image plane perpendicular to the fissure; *2DSUS* 2-dimensional sector array ultrasound

the body dimension, especially of the length. This was also the reason why 3D=LUS (used with *wideview*-mode) could not measure the length of all bodies. Secondly, the poor image quality close to the sector ultrasound probe impeded the depiction of the top layer of targets. The third reason is only an issue for the resolution measurements. The 3D-reconstructed parallel sector ultrasound (3D = SUS) was often not able to depict the thinner fissure with one-millimeter distance between the two bodies.

Referring to Table 1, iMRI provided more precise results than both two-dimensional ultrasound measurements (2DSUS and 2DLUS). In the direct comparison of the two probes, we found that linear array measurements were more precise than the corresponding ones made with the sector array probe both in 2D and in 3D mode. For all SUS measurements the spread was wider than for iMRI and all LUS measurements (see standard deviation in Table 1).

Furthermore, we found a connection between length, width and resolution results, and the image orientation while performing the 3D-scan. In contrast, height shows no marked differences between both three-dimensional measurements with the same probe. This connection was most apparent regarding 3D = SUS and 3D+SUS. Length and resolution were more exactly measured with the image plane perpendicular to the fissure between the two bodies (3D+SUS). Width was better measured with an image orientation par-

allel to the fissure (3D = SUS). It is noticeable that the poorer 3D-reconstructed results, which at the same time are closer to the 2D-measurement for length and width, were measured with the image data captured by the probe itself. The better results were reconstructed using navigation data of the image set. This correlation is also visualized in Figs. 3 and 4.

As with the sector ultrasound, the linear array measurements show a correlation of image orientation with the 2D-measurements. The same measurements are closer to the results of the 2DLUS, although the perpendicular image set (3D+LUS) always provided more exact results.

Table 1 also shows that the 3D-reconstructed linear array ultrasound provides more precise results for any measurement than the 2DLUS. Nearly all results of iMRI and 3D-LUS are in a range of less than half a millimeter around the real body dimension. Only length measured with 3D = LUS exceeds this range. The results of 3D+LUS are more precise than 3D = LUS and 2DLUS for each observed parameter. As visualized in Figs. 3 and 4, 3D+LUS measurements are close to those of iMRI. For resolution results they are even more exact than iMRI.

All measurements with the sector ultrasound probe show poorer results than iMRI and the linear array probe, except for length measured with 2DLUS versus 3D+SUS.

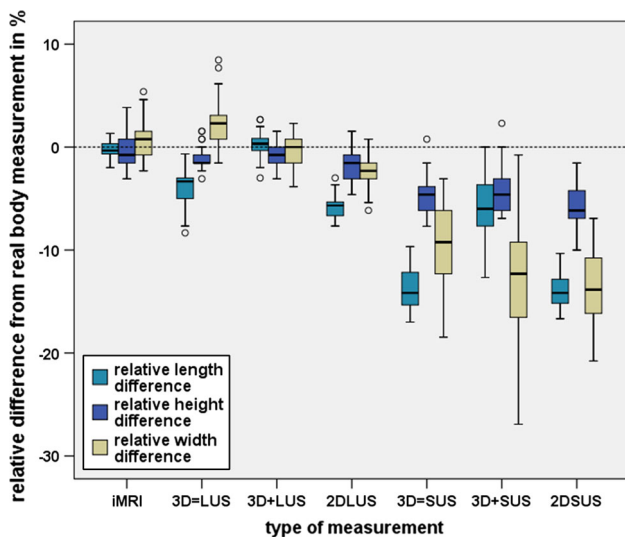


Fig. 3 Comparison of all measurement methods as relative differences from the real body dimension

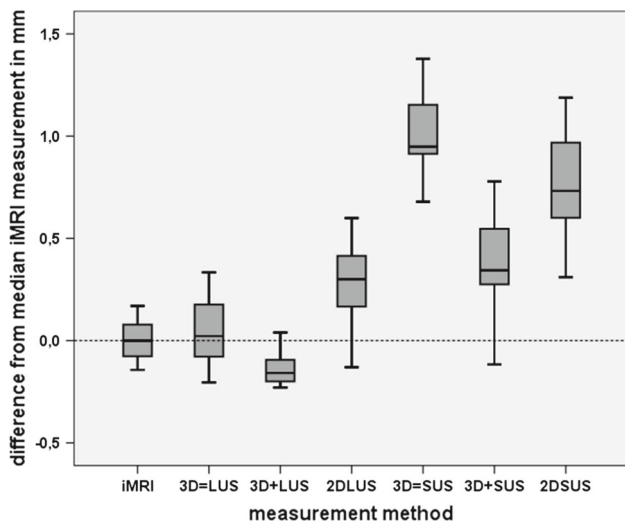


Fig. 4 In this boxplot, the absolute differences in all measurement methods to the median iMRI resolution are illustrated. The median iMRI resolution as current gold standard serves as reference (dotted line)

Figure 3 shows a comparison of all measurement methods as relative differences from the real body dimensions.

The reconstructed linear array transducer results are all clustered around the reference line with a maximum difference of 4.0% (Table 1) for length measured with 3D = LUS. Sector ultrasound results always overestimated the body dimensions up to 13.9% (Length measured with 3D = SUS).

Figure 4 illustrates the absolute differences in resolution of all measurement methods to the median iMRI resolution in a boxplot. The results of iMRI are clustered around the reference line as the median resolution of the current gold standard serves as the reference. The resolution differences

of 3D = LUS are close to those of iMRI, while 3D+LUS exceeds the resolution limit of iMRI. Both two-dimensional and the 3D-reconstructed SUS measurements offer a poorer resolution than iMRI and the 3D-reconstructed LUS.

Discussion

Since Gronningsaeter et al. [19] integrated ultrasound imaging into a modern neuronavigation system, there has been a growing number of studies examining the use of ultrasound imaging in brain tumor surgery. Navigated ultrasound has proven itself valuable for intraoperative brain shift control [12–15]. The use of small, shaped probes inside the resection cavity showed a good visualization and differentiation of edema, pathologic and normal brain tissue, and improved resection control by ultrasound [16,17,20]. Moiyadi et al. used modern navigated 3D-ultrasound as standalone intraoperative imaging [21].

Despite these clinical studies, which mostly demonstrated a positive applicability of ultrasound in brain tumor surgery, to date, no data examining the accuracy and resolution of modern navigated ultrasound probes have been found. Furthermore, few studies exist in which modern ultrasound devices are compared to other intraoperative imaging techniques like intraoperative MRI.

The aim of this study was to fill this gap in empirical research with data ascertained using an experimental phantom mimicking the features of brain tissue with an embedded tumorous lesion. The measurements of two different modern ultrasound probes were compared to MRI in an intraoperative setting.

Accuracy of the methods used

CT, iMRI and iUS measurements were possible without significant impairment of image quality. Reference data for resolution are only available for the LUS probe (L15-7io used on an iU22). Our data showed a resolution of 0.57 mm at a set penetration depth of 5 cm. Reference data by Moran et al. showed a highly comparable resolution of 0.6 mm for the full range of depth and a resolution of 0.53 mm for a depth of 0–10 mm [22].

Comparison of linear and sector array measurements

We found a clear superiority of the resolution and accuracy of LUS compared to SUS. The best results of SUS are only close to the poorest LUS results regarding length (2DLUS vs. 3D+SUS) and resolution (2DLUS vs. 3D+SUS). These experimental data correspond with previous clinical findings of our group assessing sensitivity and specificity for resid-

ual tumor detection during LGG and HGG surgery [16,17]. Since these studies did not measure the exact extent of residual tumor but assessed histopathologic findings around the resection cavity, a direct comparison of the data was not possible. Yet, ROC tests revealed a “poor” accuracy of the 2DSUS transducer, whereas the 2DLUS transducer reaches a “fair” accuracy.

The three-dimensionally reconstructed images almost always provided more accurate results than the 2D-measurements. One reason for this superiority of 3D-reconstructed results might be the better image quality of navigated ultrasound described by Renovanz et al. [10]. Another factor that might have a positive influence on the results is the reconstruction algorithm, since it fills the voxels of the volume with the surrounding data and extrapolates the end of the fissure in certain situations.

Another interesting finding of the three-dimensional measurements is the connection between length, width and resolution results, and the image orientation. It is noticeable that the 3D-results measured with the image data captured by the probe itself (length in 3D=, width in 3D+) are closer to the two-dimensional results of the same probe. For SUS the better results are reconstructed out of the navigation data of the entire image set (width in 3D = SUS, length in 3D+SUS). Regarding linear array ultrasound, 3D+LUS is more exact than 3D = LUS for each investigated variable. This leads to the assumption that the reconstruction based on an accumulation of several 2D ultrasound images provides more exact values than the fanned-out SUS image or the angled part of the *wideview*-image of the LUS probe.

For both probes, height measurements provided comparable results with all measurements (2D, perpendicular and parallel), within the same probe. This measure can be regarded as a control since height is not affected by the scan direction. We found a variance of less than 0.3 mm within the three height measurements of each probe, resulting in a considerably low error of measurement in our series.

Lindseth et al. [23] investigated the pinpoint accuracy of a phased array navigated ultrasound system (*SonoWand*[®], *MISON AS, Norway*), examining a wire phantom in a water bath. They obtained average differences in measurements of 0.05 mm (Y- and Z-axis) and 0.21 mm (X-axis) for 50 mm each, which is relatively similar to the results of the linear array ultrasound in our study. Although the results cannot be directly compared, because they did not separate their results in different sweep directions and acquisition moves (tilt scan or translation sweep), they also show a relation to the X- and Y-axes, representing length and width. As in our data, height also showed the smallest differences and standard deviation.

Comparison of linear array ultrasound and iMRI

The results of iMRI and the 3D-reconstructed measurements with the linear array probe were all clustered around the real body dimension. They differed in a small range of 0.2–4.0% to the real body dimension. The resolution limit was once higher and once lower than iMRI, depending on the image orientation during data acquisition. 2DLUS overestimated the real body dimension of up to 5.9%, and the resolution limit was nearly twice as high as the one of iMRI and the 3D-reconstructed LUS. Considering the results of the above-mentioned clinical results of our group [16,17], this difference in 3D-LUS compared to iMRI might not be of significance during surgery as a specificity and sensitivity for residual tumor detection of 2DLUS close or even better than iMRI was described.

Comparison of sector array ultrasound and iMRI

In our experimental study, all SUS measurements showed an inferior resolution compared to iMRI and overestimated the real body dimensions by up to 13.9%. Taking into consideration that SUS could not depict the topmost targets, our data resemble that of the clinical study of Gerganov et al. after resection [9]. Visualization of small or superficial residual tumor pieces with sector array ultrasound was described as being difficult to generate, caused by decreasing image quality and artifacts occurring during resection.

Contrary to the above-mentioned differences between SUS and MRI, an experimental animal study of Sheng et al. [24] showed no significant differences. They measured the volume after splenic microwave ablation with a phased array 3D-reconstructed ultrasound and MRI.

Our results of measurement inaccuracies are smaller than the differences reported for other sources of error in brain tumor surgery such as brain shift and other sources of patient to image registration inaccuracies [23,25–27].

Limitations

We were unable to determine the exact speed of sound in our gel mixtures. An agarose concentration of 2% was described to have acoustic properties close to human tissue [28]. As a result, we used concentrations close to this ratio.

Temperature and the use of backscattering material could also have had an influence on the speed of sound and, as a consequence, on the accuracy of the ultrasound. The speed of sound has an influence on measurements in propagation direction of the ultrasound beam. In linear array transducers, it influences measurement of height. Width and length measurements are influenced in sector array transducer and in *wideview*-parts of the used linear array transducer caused by the angled propagation direction. Other

sources of error using ultrasound devices are the quality loss caused by data transfer between the navigation software and the ultrasound device [19] as well as errors caused by the calibration process [23,29]. Another limitation is the ultrasound reconstruction algorithm that was used, due to the fact that there have been more accurate algorithms developed in recent years than the PNN algorithm used by our software [30,31].

Another point to be mentioned concerning iMRI is the loss of accuracy by distortions outside of the isocenter [32,33].

The results of the 3D measurements cannot be transferred directly to the clinical routine. Our study represents an ideal experimental setup. During surgery, ultrasound scanning is limited by the shape of the situs and the resection cavity which significantly impairs the quality of image reconstruction. During the course of surgery, several artifacts might accumulate, significantly impairing the quality of US images [9,34].

Future perspectives and clinical implications

Our data on 3D reconstruction from an experimental setup are not per se transferable to the clinical routine. Usually irregularly shaped resection cavities have to be assessed. Thus, usually a slightly fanned acquisition scan has to be performed leading to a drop of resolution in regions distant to the probe. Attenuation artifacts will further impair the scanning results. Intraoperative MRI is not as prone to artifacts as iUS. Hence, it is very important to make a comparison in a clinical setup to assess whether the advantages of linear array ultrasound hold true for a non-experimental setup. Surgeons using 3D-reconstructed ultrasound should be aware of the correlation of the resolution and accuracy with the image orientation while data acquisition.

Conclusion

In an experimental setup, modern intraoperative linear array ultrasound provides an accuracy comparable to MRI in an intraoperative setting. The accuracy of conventional sector ultrasound is significantly poorer than iMRI and linear array ultrasound. 3D reconstruction in the current experimental setup has the potential to improve accuracy of ultrasound images, though there is a strong dependence on image orientation during data acquisition.

Compliance with ethical standards

Conflict of interest Jan Coburger and Ralph König work as consultants for Brainlab and have received speaker fees. The other authors have declared no personal conflict of interest.

References

- Sanai N, Berger MS (2008) Glioma extent of resection and its impact on patient outcome. *Neurosurgery* 62:753–764 (discussion 264–6)
- Oszwald A, Guresir E, Setzer M, Vatter H, Senft C, Seifert V, Franz K (2012) Glioblastoma therapy in the elderly and the importance of the extent of resection regardless of age. *J Neurosurg* 116:357–364
- Hervey-Jumper SL, Berger MS (2014) Role of surgical resection in low- and high-grade gliomas. *Curr Treat Options Neurol* 16:284–014-0284-7
- Nimsky C, Ganslandt O, Buchfelder M, Fahlbusch R (2006) Intraoperative visualization for resection of gliomas: the role of functional neuronavigation and intraoperative 1.5 T MRI. *Neurol Res* 28:482–487
- Unsgaard G, Rygh OM, Selbekk T, Muller TB, Kolstad F, Lindseth F, Hernes TA (2006) Intra-operative imaging with 3D ultrasound in neurosurgery. *Acta Neurochir (Wien)* 148:235–253
- Coburger J, Nabavi A, König R, Wirtz CR, Pala A (2017) Contemporary use of intraoperative imaging in glioma surgery: a survey among EANS members. *Clin Neurol Neurosurg* 163:133–141
- Zhang G, Li Z, Si D, Shen L (2017) Diagnostic ability of intraoperative ultrasound for identifying tumor residual in glioma surgery operation. *Oncotarget* 8:73105–73114
- Mahboob SO, McPhillips R, Qiu Z, Jiang Y, Meggs C, Schiavone G, Button T, Desmulliez M, Demore CE, Cochran S, Eljamel S (2016) Intraoperative ultrasound (IoUS) guided resection of gliomas: a meta-analysis and review of the literature. *World Neurosurg* 92:255–263
- Gerganov VM, Samii A, Giordano M, Samii M, Fahlbusch R (2011) Two-dimensional high-end ultrasound imaging compared to intraoperative MRI during resection of low-grade gliomas. *J Clin Neurosci* 18:669–673
- Renovanz M, Hickmann AK, Henkel C, Nadji-Ohl M, Hopf NJ (2014) Navigated versus non-navigated intraoperative ultrasound: is there any impact on the extent of resection of high-grade gliomas? A retrospective clinical analysis. *J Neurol Surg A Cent Eur Neurosurg* 75:224–230
- Unsgaard G, Ommedal S, Muller T, Gronningsaeter A, Nagelhus Hernes TA (2002) Neuronavigation by intraoperative three-dimensional ultrasound: initial experience during brain tumor resection. *Neurosurgery* 50:804–812
- Rasmussen IA Jr, Lindseth F, Rygh OM, Berntsen EM, Selbekk T, Xu J, Nagelhus Hernes TA, Harg E, Haberg A, Unsgaard G (2007) Functional neuronavigation combined with intra-operative 3D ultrasound: initial experiences during surgical resections close to eloquent brain areas and future directions in automatic brain shift compensation of preoperative data. *Acta Neurochir (Wien)* 149:365–378
- Ohue S, Kumon Y, Nagato S, Kohno S, Harada H, Nakagawa K, Kikuchi K, Miki H, Ohnishi T (2010) Evaluation of intraoperative brain shift using an ultrasound-linked navigation system for brain tumor surgery. *Neurol Med* 50:291–300
- Riva M, Hennersperger C, Milletari F, Katouzian A, Pessina F, Gutierrez-Becker B, Castellano A, Navab N, Bello L (2017) 3D intra-operative ultrasound and MR image guidance: pursuing an ultrasound-based management of brainshift to enhance neuronavigation. *Int J Comput Assist Radiol Surg* 12:1711–1725
- Prada F, Del Bene M, Mattei L, Lodigiani L, DeBeni S, Kolev V, Vetrano I, Solbiati L, Sakas G, DiMeco F (2015) Preoperative magnetic resonance and intraoperative ultrasound fusion imaging for real-time neuronavigation in brain tumor surgery. *Ultraschall Med* 36:174–186
- Coburger J, Scheuerle A, Kapapa T, Engelke J, Thal DR, Wirtz CR, König R (2015) Sensitivity and specificity of linear array intraop-

- erative ultrasound in glioblastoma surgery: a comparative study with high field intraoperative MRI and conventional sector array ultrasound. *Neurosurg Rev* 38:499–509
17. Coburger J, Scheuerle A, Thal DR, Engelke J, Hlavac M, Wirtz CR, König R (2015) Linear array ultrasound in low-grade glioma surgery: histology-based assessment of accuracy in comparison to conventional intraoperative ultrasound and intraoperative MRI. *Acta Neurochir* 157:195–206
 18. Coburger J, König RW, Scheuerle A, Engelke J, Hlavac M, Thal DR, Wirtz CR (2014) Navigated high frequency ultrasound: description of technique and clinical comparison with conventional intracranial ultrasound. *World Neurosurg* 82(3–4):366–375
 19. Gronningsaeter A, Kleven A, Ommedal S, Aarseth TE, Lie T, Lindseth F, Lango T, Unsgard G (2000) SonoWand, an ultrasound-based neuronavigation system. *Neurosurgery* 47:1373–1379 (discussion 1379–80)
 20. Serra C, Stauffer A, Actor B, Burkhardt JK, Ulrich NH, Bernays RL, Bozinov O (2012) Intraoperative high frequency ultrasound in intracerebral high-grade tumors. *Ultraschall Med* 33:E306–12
 21. Moiyadi AV, Shetty P (2016) Direct navigated 3D ultrasound for resection of brain tumors: a useful tool for intraoperative image guidance. *Neurosurg Focus* 40:E5
 22. Moran CM, Pye SD, Ellis W, Janeczko A, Morris KD, McNeilly AS, Fraser HM (2011) A comparison of the imaging performance of high resolution ultrasound scanners for preclinical imaging. *Ultrasound Med Biol* 37:493–501
 23. Lindseth F, Lango T, Bang J, Nagelhus Hernes TA (2002) Accuracy evaluation of a 3D ultrasound-based neuronavigation system. *Comput Aided Surg* 7:197–222
 24. Sheng L, Li J, Chen J, Liang P, Dong B (2015) Comparison of 3D ultrasound and magnetic resonance imaging for microwave ablation in the canine splenomegaly model. *Int J Comput Assist Radiol Surg* 10:459–464
 25. Bayer S, Maier A, Ostermeier M, Fahrigr R (2017) Intraoperative imaging modalities and compensation for brain shift in tumor resection surgery. *Int J Biomed Imaging* 2017:6028645
 26. Stieglitz LH, Fichtner J, Andres R, Schucht P, Krahenbuhl AK, Raabe A, Beck J (2013) The silent loss of neuronavigation accuracy: a systematic retrospective analysis of factors influencing the mismatch of frameless stereotactic systems in cranial neurosurgery. *Neurosurgery* 72:796–807
 27. Gerard IJ, Kersten-Oertel M, Petrecca K, Sirhan D, Hall JA, Collins DL (2017) Brain shift in neuronavigation of brain tumors: a review. *Med Image Anal* 35:403–420
 28. Zell K, Sperl JJ, Vogel MW, Niessner R, Haisch C (2007) Acoustical properties of selected tissue phantom materials for ultrasound imaging. *Phys Med Biol* 52:475–484
 29. Prager RW, Rohling RN, Gee AH, Berman L (1998) Rapid calibration for 3-D freehand ultrasound. *Ultrasound Med Biol* 24:855–869
 30. Miller D, Lippert C, Vollmer F, Bozinov O, Benes L, Schulte DM, Sure U (2012) Comparison of different reconstruction algorithms for three-dimensional ultrasound imaging in a neurosurgical setting. *Int J Med Robot* 8:348–359
 31. Cong W, Yang J, Ai D, Song H, Chen G, Liang X, Liang P, Wang Y (2017) Global patch matching (GPM) for freehand 3D ultrasound reconstruction. *Biomed Eng Online* 16:124-017-0411-2
 32. Torfeh T, Hammoud R, Perkins G, McGarry M, Aouadi S, Celik A, Hwang K, Stancanello J, Petric P, Al-Hammadi N (2016) Characterization of 3D geometric distortion of magnetic resonance imaging scanners commissioned for radiation therapy planning. *Magn Reson Imaging* 34:645–653
 33. Wang D, Strugnell W, Cowin G, Doddrell DM, Slaughter R (2004) Geometric distortion in clinical MRI systems part I: evaluation using a 3D phantom. *Magn Reson Imaging* 22:1211–1221
 34. Selbekk T, Jakola AS, Solheim O, Johansen TF, Lindseth F, Reinertsen I, Unsgard G (2013) Ultrasound imaging in neurosurgery: approaches to minimize surgically induced image artefacts for improved resection control. *Acta Neurochir (Wien)* 155:973–980